

Supporting Information

High-performance UV Photodetector with Superior Responsivity Enabled by a Synergistic Photo/Thermal Enhancement of Localized Surface Plasmon Resonance

Luxia Zheng^a, Yang Yang^{a,}, Chris R. Bowen^b, Lan Jiang^a, Zhan Shu^a, Yun He^a,
Hongli Yang^a, Zongzhuo Xie^a, Taixu Lu^a, Feng Hu^{a,*} and Weiyu Yang^a*

^aInstitute of Micro/Nano Materials and Devices, Ningbo University of
Technology, Ningbo 315211, P. R. China

^b Department of Mechanical Engineering, University of Bath, BA2 7AK, UK

*Corresponding authors

Email: yangyangafterglow@yeah.net (Yang Yang); hf17@tsinghua.org.cn (Feng
Hu)

Experimental section

Materials synthesis.

The TiO₂ nanofibers (NFs) were prepared as follows: 350 mg of polyvinylpyrrolidone (PVP) was dispersed into 3 g of anhydrous ethanol, sonicated until complete dissolution, and then 1.5 g of tetrabutyl titanate and 0.5 g of acetic acid solution was added. The solution was then placed on a magnetic stirrer and stirred vigorously for 8 h. The stirred solution was used as the precursor solution, which was electrostatically spun at 10 kV with a speed of 0.1 mm/min. The sample obtained by electrostatic spinning was placed in a ceramic crucible and calcined in a muffle furnace at 550 °C for 2 h to obtain the TiO₂ NFs.

Preparation of W₁₈O₄₉/TiO₂ composite: 25 mg of tungsten hexacarbonyl powder was weighed into 20 ml of anhydrous ethanol and stirred for 20 min, then 15 mg of TiO₂ NFs was added, and the mixture was stirred for 10 min and then placed into a sonicator for 10 min to completely dissolve the TiO₂ nanofibers, and finally, the mixture was stirred for 10 min using a magnetic stirrer. The reaction kettle was transferred into a polytetrafluoroethylene reactor, and then the reaction kettle was transferred into an oven at 160 °C for 12 h. After the temperature of the reaction kettle was reduced to room temperature, the reaction kettle was removed and subsequently washed by centrifugation with anhydrous ethanol for three times to obtain the W₁₈O₄₉/TiO₂ composites.

Equipment manufacturing and measurement.

The photodetector was constructed based on a single W₁₈O₄₉/TiO₂ nanofiber. The quartz glass was first cleaned by ultrasonically washing it for 15 minutes with neutral detergent, deionized water, and acetone. After that, it was cleaned for 10 minutes with a UV-ozone cleaning agent. The prepared W₁₈O₄₉/TiO₂ nanofibers were then dissolved in ethanol and diluted until a colorless solution was obtained. The synthesis solution was then spin cast for four minutes at a speed of 2000 rpm on a quartz substrate, and it was dried for thirty minutes at room temperature. After that, 10 μm gold electrodes were deposited at both ends of the nanorods using photolithography, thermal

evaporation, and lifting and separation processes, with a resolution of approximately 10 μm .

Characterization methods.

X-ray powder diffraction (XRD, D8 Advance, Bruker, Germany) with Cu $K\alpha$ radiation ($\lambda=1.5406 \text{ \AA}$) was employed to analyze the phase structure of the samples. Scanning electron microscopy (SEM, S-4800, Hitachi, Japan) and transmission electron microscopy (TEM, JEOL JEM-2100, Japan) were used to observe the morphology and structure of the samples. X-ray photoelectron spectroscopy (XPS, Thermo ESCALAB 250Xi, USA)) was performed with a source of Mg $K\alpha$ ADES ($h = 1253.6 \text{ eV}$) and a residual gas pressure below 10^{-8} pa. UV-Vis-IR absorption spectra of the samples were recorded on a Lambda 750 UV-Vis-IR spectrophotometer (U-3900, HITACHI, Japan).

Photoelectric Property Measurement.

Electrical and optoelectronic measurements of the produced devices was carried out on a four-probe station using a semiconductor characterization system (4200-CSC, Keithley, USA), whose data were recorded with a computer via a Labview application. The four-probe station's optical microscope aimed a laser spot to measure the performance toward the center of the as-assembled photodetector. A 500 W xenon arc lamp was used as the light source, which was connected to an Acton Research monochromator with order-sorting filters. With a laser spot size of 4 mm and fixed light wavelengths with variable light intensities (375 nm, $P_{\text{max}} = 60 \text{ mW}$), the photocurrent was measured using an Optical Power Meter (PS10, Coherent, USA). All experiments were performed at room temperature under ambient conditions.

Finite-element modeling simulations.

In this work, Finite-element modeling (FEM) calculations was employed using a commercial FEM software package to simulate electric field and the sum of the scattered fields of the simplified model is calculated at $3 \times 10^8 / 375 \times 10^{-9}$ ultraviolet frequency. The background field of the plane wave is solved by the fluctuating optical module, and the equation utilized is as follows:

$$E_b = E_0 e^{i(\omega t - k \cdot r)}$$

In the general case, k is in the xz -plane and the angle θ between k and the z -axis is given. FEM method was performed to investigate the electric field enhancement induced by LSPR of plasma nanoparticles ($W_{18}O_{49}$ NWs and $W_{18}O_{49}$ NWs/ TiO_2 NFs). In the present calculations, the $W_{18}O_{49}$ NWs/ TiO_2 NFs heterostructure system is simplified to a single $W_{18}O_{49}$ NWs (diameter $D_1 = 30$ nm) and single TiO_2 NF (diameter $D_2 = 240$ nm), where the appropriate size was selected in order to graphically express the relative position of the two components. The incident light propagated from the Y -direction and polarized light (375 nm) along the Z -direction, and a cover grid cell size of $1 \times 1 \times 1$ nm³ was used.

Supplementary Figures

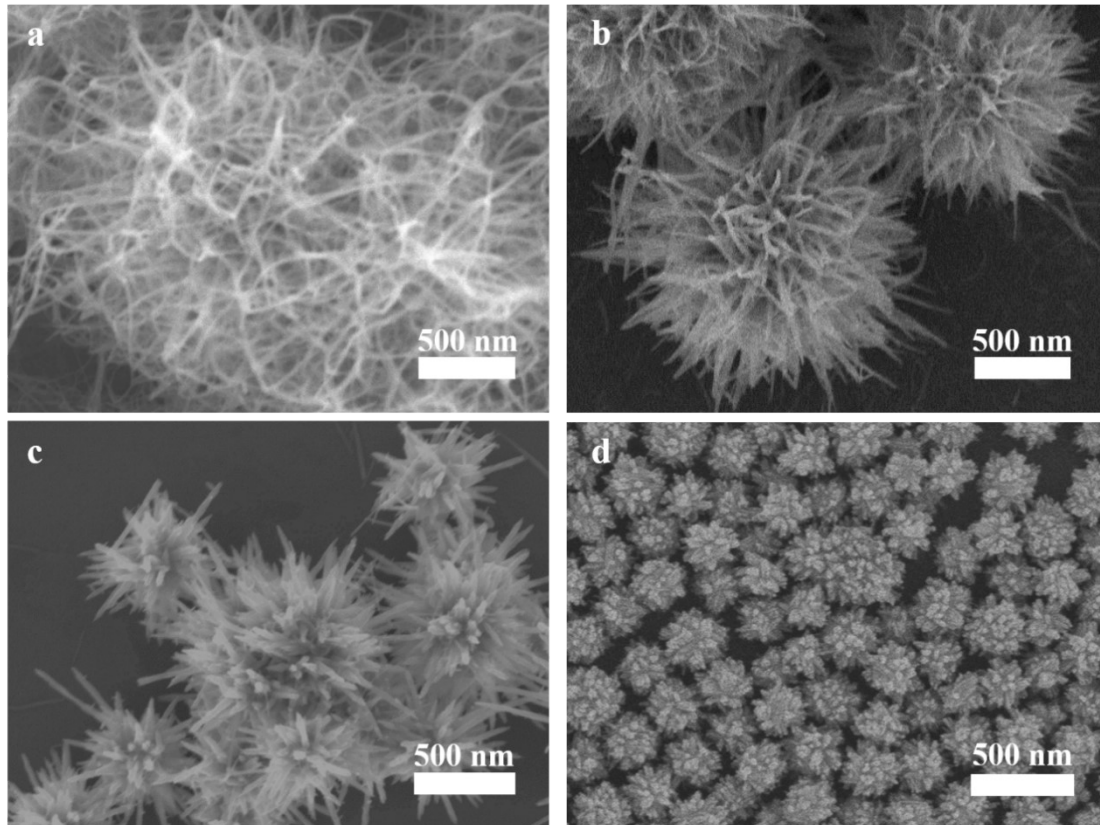


Figure S1 TEM image of $W_{18}O_{49}$ NWs after hydrothermal treatment at different temperatures: (a) 140°C; (b) 160°C; (c) 170°C; (d) 180°C.

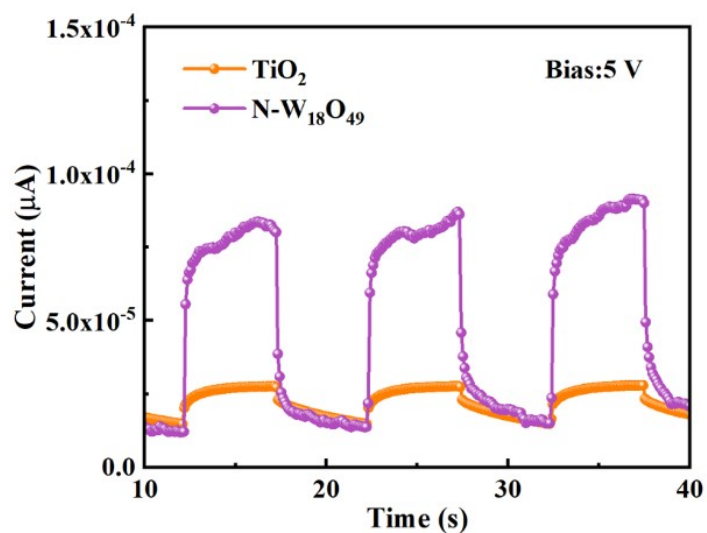


Figure S2. On/off switching characterization of the TiO_2 and passivated $\text{W}_{18}\text{O}_{49}/\text{TiO}_2$ under 375 nm light at a bias of 5 V.

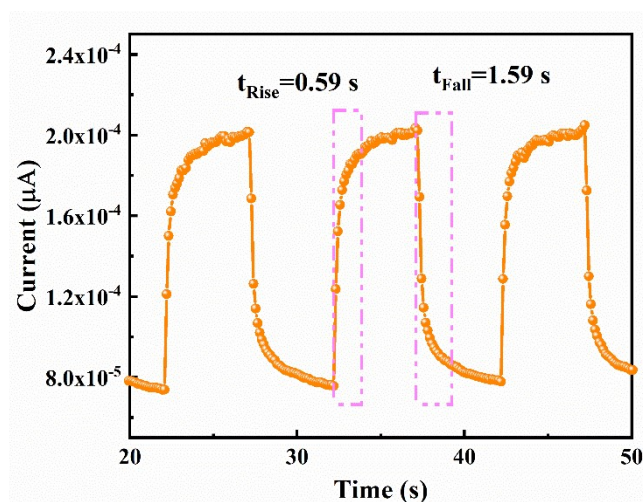


Figure S3. I - T characteristic curves of the TiO_2 photodetectors.

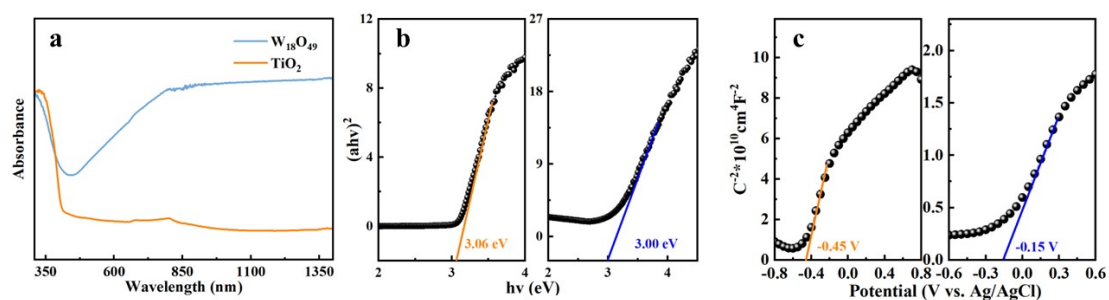


Figure S4. (a) UV-vis-IR absorption spectra of the $\text{W}_{18}\text{O}_{49}$ and TiO_2 ; b) Plots of $(ah\nu)^2$

versus $h\nu$ of the TiO_2 NFs and $\text{W}_{18}\text{O}_{49}$ NWs; (c) Mott-Schottky plots of the TiO_2 NFs and $\text{W}_{18}\text{O}_{49}$ NWs.